

Animal Cells and Systems

ISSN: 1976-8354 (Print) 2151-2485 (Online) Journal homepage: www.tandfonline.com/journals/tacs20

Autophagy-driven MHC-I downregulation enables NK cell-mediated clearance of intracellular uropathogenic *E. coli* in urinary tract infection

Manisha Naskar, Gyeongseo Suk, Hana Yoon, Donghoon Lim, Soman N. Abraham & Hae Woong Choi

To cite this article: Manisha Naskar, Gyeongseo Suk, Hana Yoon, Donghoon Lim, Soman N. Abraham & Hae Woong Choi (2026) Autophagy-driven MHC-I downregulation enables NK cell-mediated clearance of intracellular uropathogenic *E. coli* in urinary tract infection, Animal Cells and Systems, 30:1, 1-19, DOI: 10.1080/19768354.2025.2588910

To link to this article: https://doi.org/10.1080/19768354.2025.2588910

© 2025 The Author(s). Published by Informa UK Limited, trading as Taylor & Francis Group

View supplementary material

Published online: 01 Dec 2025.

Submit your article to this journal

Article views: 448

View related articles

View Crossmark data

Full Terms & Conditions of access and use can be found at
https://www.tandfonline.com/action/journalInformation?journalCode=tacs20

ANIMAL CELLS AND SYSTEMS
2026, VOL. 30, NO. 1, 1–19
https://doi.org/10.1080/19768354.2025.2588910

Taylor & Francis
Taylor & Francis Group

OPEN ACCESS Check for updates

Autophagy-driven MHC-I downregulation enables NK cell-mediated clearance of intracellular uropathogenic *E. coli* in urinary tract infection

Manisha Naskar[a], Gyeongseo Suk[a], Hana Yoon[b], Donghoon Lim[c], Soman N. Abraham[d] and Hae Woong Choi [a]

[a]Division of Life Sciences, Korea University, Seoul, South Korea; [b]Department of Urology, Ewha Womans University, College of Medicine, Seoul, South Korea; [c]Department of Urology, Chosun University School of Medicine, Gwangju, South Korea; [d]Department of Pathology, Duke University Medical Center, Durham, NC, USA

ABSTRACT

Uropathogenic *E. coli* (UPEC) accounts for over 80% of urinary tract infections (UTIs) due to its distinct capacity to invade and persist within bladder epithelial cells (BECs). The ability of UPEC to survive for extended periods within BECs can also contribute to the recurrence of UTIs. Since natural killer (NK) cells are part of the innate immune defense with a unique capacity to kill intracellular bacteria, we aimed to examine the potential role of these cells in bacterial clearance during UTIs. Here, we report that infecting mouse bladders with UPEC promoted a significant recruitment of NK cells to UPEC-infected BECs. Depletion of NK cells using neutralizing antibodies increased the bacterial load in the infected bladder, indicating a protective role for NK cells against the host. Co-culturing BECs harboring intracellular UPECs with NK cells in vitro significantly reduced the intracellular bacterial burden in BECs. The targeting of infected BECs by NK cells required reduced major histocompatibility complex (MHC) class I (MHC-I) expression, an inhibitory signal on NK cells, a process facilitated by autophagy, and concurrent increased CD48 expression on BECs, a ligand that activates NK cells. The recruitment of NK cells to UPEC-infected BECs was mediated by chemokines CXCL10 and CXCL12. Administering the IL-15/IL-15Rα supercomplex, a potent activator of NK cells, to UPEC-infected mice significantly reduced the bacterial load in the bladder. These observations highlight NK cells as an overlooked component in the innate immune defense against UTIs and a potential therapeutic target.

ARTICLE HISTORY
Received 29 July 2025
Revised 19 September 2025
Accepted 10 October 2025

KEYWORDS
NK cell; MHC-I lysosomal degradation; urinary tract infection; CD48; host pathogen interaction

Introduction

Uropathogenic *E. coli* (UPEC) accounts for approximately 85% of uncomplicated urinary tract infections (UTIs) (Foxman and Brown 2003). Upon entering the bladder via the urethra and multiplying in urine, UPEC adheres avidly to uroplakin plaques on the apical surface of superficial bladder epithelial cells (BECs). UPEC adherence is mediated by hair-like structures called fimbriae, which contain a mannose-binding protein, FimH, at their tips, facilitating strong binding to uroplakin components (Abraham et al. 1985), while also allowing the BECs to resist expulsion during voiding. A significant number of these adherent UPEC subsequently enter the normally impermeable superficial bladder epithelium and become encapsulated within intracellular Rab27$^+$ fusiform vesicles (Chen et al. 2003). Consequently, UPEC evades removal during voiding and escapes elimination by phagocytic cells, which are typically recruited to clear infections (Justice et al. 2006). This ability to persist within BECs, beyond the reach of immune cells and antibiotics, is a major factor contributing to UPEC survival and recurrent infections.

However, several innate bladder immune responses exist to counter this invasion of the bladder epithelial barrier by UPEC. Indeed, one response involves the spontaneous expulsion of Rab27b$^+$ vesicles containing intracellular bacteria from the apical surfaces of BECs, which occurs through various exocytic and intracellular trafficking mechanisms present in BECs, including a TRPML3-dependent pathway (Miao et al. 2015). When

CONTACT Hae Woong Choi haewoongchoi@korea.ac.kr Hana Science Bldg, #513, 145 Anamro, Seongbuk-gu, 02841 Seoul, South Korea
Supplemental data for this article can be accessed online at https://doi.org/10.1080/19768354.2025.2588910

© 2025 The Author(s). Published by Informa UK Limited, trading as Taylor & Francis Group
This is an Open Access article distributed under the terms of the Creative Commons Attribution-NonCommercial License (http://creativecommons.org/licenses/by-nc/4.0/), which permits unrestricted non-commercial use, distribution, and reproduction in any medium, provided the original work is properly cited. The terms on which this article has been published allow the posting of the Accepted Manuscript in a repository by the author(s) or with their consent.

the bacterial burden in BECs becomes particularly high, mast cells in the lamina propria are recruited to the superficial epithelium, which then degranulate and induce widespread exfoliation of infected BECs. This substantial loss of infected BECs can promote more than 90% reduction in bacterial load within the bladder (Choi et al. 2016; Naskar and Choi 2024).

Despite the presence of multiple bacteria-clearing mechanisms in the bladder, initial and recurrent UTIs remain prevalent, even among healthy individuals. This persistence is largely attributable to the ability of a small population of UPEC to evade immune clearance by establishing intracellular reservoirs within BECs (Anderson et al. 2003). Thus, instead of being completely eradicated, UPEC exploits host intracellular trafficking pathways to shuttle between compartments within BECs (Mysorekar and Hultgren 2006; Naskar et al. 2023). Initially, UPEC appears to be sequestered within Rab27B^{+} vesicles, a compartment associated with exocytic pathways; however, when not promptly expelled, UPEC persists within intracellular compartments that exhibit autolysosome-like characteristics (Naskar et al. 2023). These autolysosome-like structures provide UPEC with a protective niche, facilitating survival despite the host defense mechanisms. This intracellular persistence also likely contributes to the high rate of UTI recurrence and complicates complete bacterial clearance, even with antibiotic treatment.

Natural killer (NK) cells are immune cells that have been largely overlooked in relation to UTIs, yet are associated with chronic and recurrent infections, and play a crucial role in immune defense by targeting and eliminating infected host cells. Upon arriving at infected sites, NK cells are programmed to recognize major histocompatibility complex (MHC) class I (MHC-I) molecules on host cells, thereby distinguishing and sparing healthy cells (Kärre et al. 1986; Koch et al. 2013). However, when MHC-I expression is downregulated – a common response to viral infection – NK cells promptly release cytotoxic granules containing perforin and granzymes to eliminate these affected cells. In addition to downregulating MHC-I, many infected host cells upregulate ligands that activate NK cells, such as MICA, MICB, ULBPs, B7-H6, CD48, and nectin-2 (Kärre et al. 1986). These ligands enhance NK cell cytotoxic activity by engaging complementary receptors on NK cell surfaces, including NKG2D, NKp30, NKp44, NKp46, and 2B4 (Koch et al. 2013).

The current understanding regarding whether NK cells play a role in clearing UPEC-infected BECs during UTIs remains limited. Here, to our knowledge, we reveal for the first time that NK cells are recruited to UTI sites through the local release of cytokines and contribute significantly to the clearance of bacteria-infected BECs. We demonstrate that NK cells have the capacity to distinguish between infected and uninfected BECs, and that the elimination of NK cells greatly enhances the bacterial burden in the bladder.

Materials and methods

Bacterial strain

In vitro and in vivo infections were conducted using the UPEC CI5 strain. UPEC were cultivated in Luria–Bertani broth at 37 °C under static conditions for 14–18 h. Bacterial colonies were quantified by plating on MacConkey agar plates and then incubating at 37 °C overnight.

In vitro bladder cell line and in vivo mouse study

The human BEC line 5637 (ATCC HTB-9) was cultured in RPMI media (Gibco) supplemented with 10% fetal bovine serum (FBS), 10 mM HEPES, 1 mM sodium pyruvate, and 0.225% glucose. Cells were maintained in a 5% CO_2 incubator at 37 °C. In vivo experiments were conducted on 7–8-week-old C57BL/6J female mice (Raon Bio). Anesthetized mice were infected transurethrally with 1×10^8 UPEC colony-forming units (CFUs). At 6 h post-infection, ciprofloxacin (200 mg/kg) was administered intraperitoneally (i.p.) in phosphate-buffered saline (PBS). Infected mice were then sacrificed at the desired time point post-infection. Bladders were dissected and suspended in 0.1% Triton X-100, followed by homogenization using a bead-beating homogenizer. The homogenized suspension was then plated on MacConkey agar plates and incubated at 37 °C overnight. If necessary, the suspension was diluted before plating. All animal-related experimental procedures were conducted with the approval of the Korea University Institutional Animal Care and Use Committee (IACUC).

NK cell depletion and IL-15:IL-15R complex treatment in vivo

Female 7–8-week-old C57BL/6J mice were i.p. administered 200 μg of depletion antibody (InVivoMAb anti-mouse NK1.1, Cat. #BE0036). Control mice were administered the isotype control antibody (InVivoMAb mouse IgG2a isotype control, Cat. #BE0085). For IL-15:IL-15R complex treatment in vivo, recombinant mouse IL-15R αFc chimera protein, CF (R&D Systems, Cat. #551-MR) and mouse IL-15 recombinant protein (PeproTech, 210-15-50UG) were mixed in an appropriate ratio and incubated at 37 °C for 30 min. Mice were i.p. administered the complex on days 1 and 3, with day 0 being the day of transurethral UPEC infection.

Flow cytometry

Flow cytometry was employed to analyze the number of NK cells in mouse bladders. Mice were sacrificed at appropriate time points post-infection, and their bladders were harvested in Hanks' balanced salt solution (HBSS) buffer. The tissues were transferred to a lysis buffer containing 1 mg/mL collagenase, 10 mM HEPES, and 1.5% FBS. Single-cell suspensions were prepared from bladders by passing the digested tissues through a 70 μm cell straining filter (BD Biosciences). The cells were then washed with 1% bovine serum albumin (BSA) in PBS supplemented with 3% FBS and 10 mM EDTA. Blocking was performed by incubating the cells in buffer supplemented with 5% normal mouse serum, 5% normal rat serum (Jackson ImmunoResearch), and 1% Fc block (eBiosciences) for 15 min. Next, the cells were stained with the necessary antibodies at 4 °C for 30 min. Flow cytometry was performed using FACSVerse (BD) or FACSymphony A1 (BD), and the data were analyzed using FlowJo software (BD). The list of used antibodies is provided: PE–cyanine5.5 CD19 monoclonal antibody (eBioscience), FITC anti-mouse Ly6G antibody (Biolegend), PerCP–cyanine5.5 anti-mouse/human CD11b antibody (Biolegend), PE anti-mouse CD3e (Biolegend), PE–cyanine7 anti-mouse I-A/I-E antibody (Biolegend), PE–cyanine7 anti-mouse NK-1.1 antibody (Biolegend), APC anti-mouse CD11c antibody (Biolegend), APC anti-mouse CD335 (NKp46) antibody (Biolegend), APC–cyanine7 anti-mouse CD45 antibody (Biolegend).

Intracellular CFU count assay

To assess the intracellular bacterial burden, BECs were seeded at a density of 1×10^5 cells per well in a 24-well plate and incubated for 16–20 h. After incubating, the cells were infected with UPEC at the intended multiplicity of infection (MOI). The plate was then centrifuged at 1200 rpm for 5 min. After incubating for 1 h, the medium was replaced with a gentamicin-containing medium (200 μg/mL) to remove any extracellular bacteria. After 30 min, the medium was further replaced with a reduced gentamicin concentration (50 μg/mL), which was thereafter maintained. This eliminated any expelled bacteria, allowing for an intracellular bacterial count. At relevant time points, the wells were washed thrice with PBS. After washing, 0.1% Triton X-100 in PBS was added to lyse the cells. The lysate was plated onto MacConkey agar plates, and the bacterial colonies were counted to determine the number of intracellular bacteria within epithelial cells.

Immunofluorescence staining and imaging

Mouse bladders were dissected at the appropriate times post-infection. The bladder tissue was fixed in 4% paraformaldehyde and frozen in optimal cutting temperature (OCT) compound. For sectioning, a Leica Biosystems CM1850 cryostat (Leica Biosystems Inc.) was used. The sliced tissues were blocked and permeabilized in a buffer containing 0.3% Triton and 2.5% normal goat serum (Gibco) in 1% BSA–PBS. Primary antibodies against *E. coli* (BioRad), granzyme B (Cell Signaling Technology), HLA-A/B/C (Santa Cruz), LC3A/B (Cell Signaling Technology), or LAMP1 (Novus Biologicals) were added and incubated overnight. The next day, the samples were incubated with the appropriate fluorochrome-conjugated secondary antibodies (Jackson ImmunoResearch). Bladder sections were mounted using ProLong Diamond Antifade Mountant with DAPI (Invitrogen). The samples were visualized using an LSM800 microscope (Zeiss).

For in vitro imaging analyses, the BECs were seeded on round glass coverslips inserted into a 24-well plate at a density of 1×10^5 cells/well and incubated overnight. The next day, the cells were infected with UPEC at the intended MOI. A gentamicin assay was conducted along with mannose (0.5%) to ensure the removal of dead

extracellular bacteria. After incubating for 1 h, the medium was replaced with fresh medium containing gentamicin (200 µg/mL) and mannose (0.5%). After 30 min, the medium was further supplemented with gentamicin (50 µg/mL) and methyl D-mannose (0.5%), and the plates were incubated for the required time. Mannose was added to the medium to prevent UPEC from reattaching and re-entering the BECs. After appropriate time points, the cells were washed three times with 1x PBS. The cells were fixed with 4% paraformaldehyde at RT for 20 min. The fixed cells were permeabilized and blocked with 0.1% saponin (20 min) in 1% BSA for 1 h. The cells were then incubated at 4 °C with primary antibodies overnight. The following day, the cells were washed three times with a 0.5% saponin solution and treated with the appropriate fluorophore-conjugated secondary antibodies. The examination of slides was performed on a Zeiss LSM800 confocal microscope. Image processing and quantification were performed using ImageJ software.

Magnetic labeling of live bacteria

UPEC were labeled with BioMag carboxyl magnetite particles (Bangs Laboratories, BM570). The required amount of magnetic particle suspension was centrifuged at 1000 g for 1 min. The BioMag particles were washed once with distilled water (DW) and twice with 0.1 M MES buffer (2-(N-morpholino) ethanesulfonic acid, pH 5.2) using a magnetic rack (BD IMagnet, BD Biosciences, 552311). To chemically activate the particles, EDAC (1-ethyl-3 – (3-dimethylaminopropyl) carbodiimide) was added to the suspension, which was incubated on a rotator at 12 rpm and RT for 15 min. After incubation, the suspension was washed twice with 1x PBS using the magnetic rack. The BioMag particles were mixed with UPEC (0.5×10^9 CFU) in 1 mL PBS and rotated at 37 °C for 30 min. The suspension was placed on the magnetic rack, and the supernatant was replaced with 1% BSA in PBS, followed by an additional incubation at 37 °C on a rotator for 30 min. To remove any larger particles, the suspension was centrifuged at 200 g for 1 min, and the resulting suspension was used to infect the cells.

Cytotoxicity assay

Cytotoxicity following UPEC infection of BECs was measured using a CytoTox96 Non-Radioactive Cytotoxicity Assay kit (Promega). BECs were seeded in a 96-well plate at a density of 2×10^4 cells/well. The next day, BECs were infected with the intended MOI, and the plates were centrifuged at 1200 rpm for 5 min and allowed to incubate for an hour, following which a gentamicin assay was conducted. The next day, NK cells were added to the wells, centrifuged at 100 g, and incubated for 16 h. The supernatant was mixed with the colorimetric substrate in a 1:1 ratio, and then the color development was measured at 492 nm using a microplate reader. Thus, cell death was an indirect measure of the lactate dehydrogenase (LDH) concentration in the supernatant.

Transient knockdown of genes in 5637 cells

BECs were seeded at a density of 1×10^5 cells per well in a 6-well plate. After incubating overnight, the cells were transfected with various concentrations of siRNA targeting a specific gene or non-specific siRNA duplexes using Xfect Transfection Reagent (Takara Bio Company). The siRNA oligonucleotides were developed using Bionics. Transfected cells were used for assays of interest after 24–36 h. The knockdown was confirmed via western blot analysis. The used siRNA sequences are as follows:

si*NBR1*: forward: CCTGAGAGCTTGCTCCAGTCTA; reverse: CTTGGTTCCTGGCTGAAGGTGA; si*beclin1*: forward: CTGGACACTCAGCTCAACGTCA; reverse: CTCTAGTGCCAGCTCCTTTAGC; si*ATG5*: forward: GCAGATGGACAGTTGCACACAC; reverse: GAGGTGTTTCCAACATTGGCTCA.

The pEGFP-LC3 plasmid (Addgene, Plasmid #24920) was used to overexpress LC3B using ScreenFect transfection reagent (Fujifilm Wako Chemicals).

Transwell migration assay

BECs were seeded on round glass coverslips placed in a 24-well plate at a density of 1×10^5 cells/well. The next day, cells were infected with UPEC at the intended MOIs. The plates were centrifuged at 1200 rpm for

5 min and then incubated for 1 h. After 1 h of incubation, gentamicin was added to the media as described above. After 24 h, the NK cells were counted and added to a Transwell insert (pore size: 5 μm; Corning) and incubated overnight. The next day, the Transwell was removed, and the coverslips were washed with 1x PBS and fixed with 4% PFA in PBS. The fixed cells were permeabilized and blocked with 0.1% saponin in 1% BSA for 20 min. Cells were then incubated at 4 °C with primary antibodies targeting the specific proteins overnight. The following day, the cells were washed, incubated with the appropriate fluorophore-conjugated secondary antibodies, and mounted using ProLong Diamond Antifade Mountant with DAPI (Invitrogen). The slides were then examined via confocal microscopy, and the number of NK cells was manually counted.

CRISPR–Cas9 was used to generate knockouts for the cytokines CXCL9, CXCL10, and CXCL12 in BECs. Here, gRNAs (guide RNAs) targeting the gene of interest were designed using online tools to ensure specificity and minimal off-target effects. The sgRNAs were cloned into the PX459 plasmid, which contains the Cas9 nuclease, a puromycin resistance marker for selection, and promoters to drive sgRNA and Cas9 expression. Human 5637 BECs were transfected with the plasmid using the Xfect transfection kit (TakaraBio). Following transfection, cells were selected and expanded using puromycin for 3 days, followed by selection and expansion of edited cells. The used gRNAs are as follows: Hu CXCL9: forward: CAC CGT TCC AAG TCA CTC CTG TAT; reverse: AAA CAT ACA GGA GTG ACT TGG AAC; Hu CXCL10: forward: CAC CGA TTG TAG GTG GAT AGT CCC T; reverse: AAA CAG GGA CTA TCC ACC TAC AAT C; Hu CXCL12: forward: CAC CGG TCA CAA AGC GAG GCC CAA; reverse: AAA CTT GGG CCT CGC TTT GTG ACC.

Quantitative polymerase chain reaction

The cells were washed with PBS, and RNA was extracted using the TaKaRa MiniBEST Universal RNA Extraction kit, following the manufacturer's instructions. Complementary DNA (cDNA) was synthesized using the Toyobo ReverTra Ace-α kit. Thunderbird next SYBR qPCR mix and CFX384 Touch Real-Time PCR Detection System (Bristol Myers Squibb) were used to conduct qRT-PCR. Target gene RNA expressions were normalized to *glyceraldehyde 3-phosphate dehydrogenase* (*GAPDH*) expression. The data were analyzed using the $^{\Delta\Delta}$CT method. The used primers are described in Supplementary Table 1.

Statistical analysis

Data were analyzed and graphs generated using GraphPad Prism Software (v.10). In mouse experiments, each dot represents one bladder. In in vitro experiments, dots correspond to samples from two or three independent experiments. Statistical significance was assessed using either an unpaired Student's *t*-test or a one-way analysis of variance (ANOVA) followed by Tukey's multiple comparisons test. Results are presented as the mean ± SEM. Post-test significance values were defined as follows: $*p < 0.05$, $**p < 0.01$, $***p < 0.001$, $****p < 0.0001$, and ns (not significant).

Results

Recruitment of NK cells during UPEC infection in the bladder as a host defense response

To investigate the host protective function of NK cells against intracellular bacteria in BECs, we utilized a widely used UTI mouse model (Bishop et al. 2007; Miao et al. 2015). To exclusively investigate the fate of intracellular bacteria, we followed bacterial bladder infections in female C57BL/6J mice treated with ciprofloxacin to eradicate all extracellular bacteria. In this mouse model, we observed a significant reduction in bacterial burden in the mouse bladder; however, residual UPEC remained present (Figure 1A). Immunofluorescence staining of bladder tissue at 24 h post-infection revealed a notable increase in NK cell numbers in the lamina propria following UPEC infection (Figure 1B). Notably, some of the newly recruited NK cells appeared to be migrating toward the superficial epithelium of the infected bladder (white arrowheads). Flow cytometry was performed to quantify NK cell recruitment at various time points post-infection, using NK1.1^{+}, NKp46^{+}, CD45^{+}, CD3ε^{-}, and CD19^{-} as markers for NK cells (Supplementary Figure 1 and Figure 1C). NK cell infiltration of the bladder was observed as early as 4 h post-infection, peaking at 12 h before gradually declining (Figure 1C). To determine whether recruited NK cells contributed to host defense

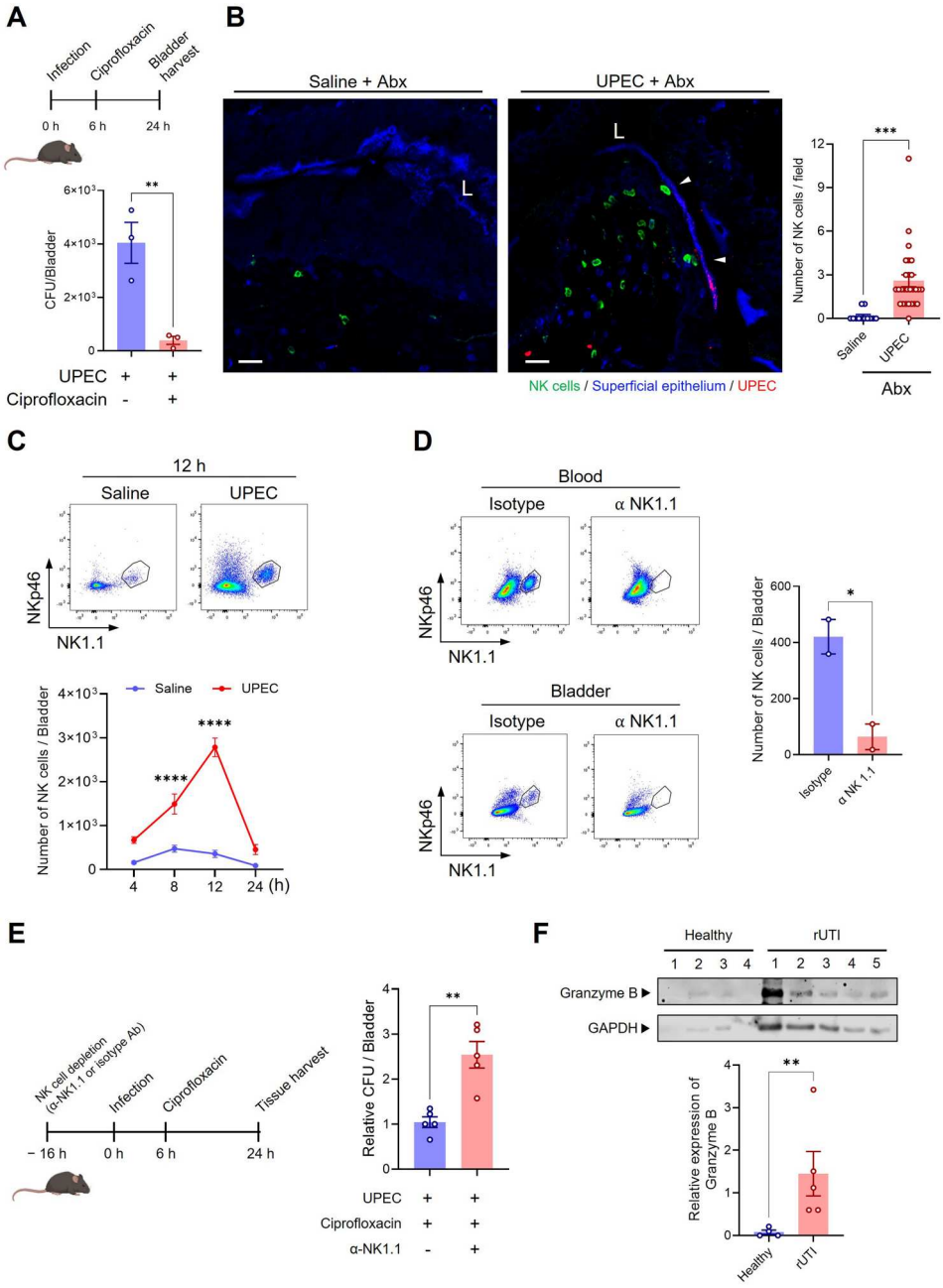


Figure 1. Recruitment of NK cells during UPEC infection in the bladder. (A, B) Residual bacterial burden after ciprofloxacin treatment and recruitment of NK cells into the infected urothelial layer. Wild-type (WT) C57BL/6J female mice were intravesically infected with the UPEC CI5 strain and administered ciprofloxacin (200 µg, Abx) 6 h post-infection, or with ciprofloxacin alone as a control. (A) At 24 h post-infection, bladder bacterial burden was examined. (B) At 24 h post-infection, sectioned bladders were stained for UPEC (red), NK cells (green), and superficial urothelium (blue). The number of NK cells per randomly chosen optical field was counted in 100 µm × 100 µm images. (C) Dynamics of NK cell recruitment in mouse bladders following UPEC infection. Female C57BL/6J mice were intravesically infected with UPEC, and bladder samples were collected at 4, 8, 12, and 24 h post-infection. NK cell presence was analyzed via flow cytometry. Each dot represents an individual mouse, with data pooled from two or three independent experiments. (D) Confirmation of NK cell depletion by flow cytometry. Mice received 200 µg of depletion antibody (anti-NK1.1 antibody) via intraperitoneal injection one day before bladder harvest for flow cytometry analysis. An isotype antibody was used for the mouse control group. (E) Increased bacterial load after NK cell depletion. Mice were administered the depletion antibody (anti-NK1.1 antibody) one day before infection. Ciprofloxacin was administered 6 h post-infection, and bladders were plated 24 h later to assess bacterial loads. (F) Detection of granzyme B in urine from UTI patients. Urine samples from UTI patients and controls were centrifuged at 13,000 rpm and 4 °C for 30 min. The supernatant was collected and analyzed for granzyme B and GAPDH expression through Western blotting.

Data are shown as the mean ± SEM. Quantitative data from two to three independent experiments were analyzed by an unpaired two-tailed Student's t-test. * $p < 0.05$; ** $p < 0.01$; *** $p < 0.001$; **** $p < 0.0001$.

against UPEC infection, we conducted an in vivo study comparing bacterial numbers in the bladder before and after NK cell depletion using an NK1.1-targeting neutralizing antibody (Figure 1D). Two groups of mice were treated with either the anti-NK1.1 antibody or the isotype control antibody, followed by bladder infection with the UPEC CI5 strain and subsequent ciprofloxacin treatment. When bacterial burdens in the bladders of the two groups were compared at 24 h post-infection, the mice treated with the NK cell-depleting antibody exhibited a significantly higher bacterial burden than the control mice (Figure 1E). Thus, NK cells play a crucial role in host defense against intracellular UPEC in the bladder.

To provide clinical support for our murine studies, we examined the urine of a limited number of symptomatic, uncomplicated UTI patients for the presence of NK activation markers and compared the marker levels with those obtained from healthy subjects. The detection of NK cell activation markers, such as granzymes, in human urine has been previously reported (Yannaraki et al. 2006). Western blotting identified that urine samples from all UTI patients contained varying levels of granzyme B, whereas none of the urine samples from healthy subjects appeared to contain this NK cell product (Figure 1F). These findings suggest a potential role for NK cells in combating UTIs in humans.

NK cells directly interact with UPEC-infected BECs to reduce bacterial burden

The recruitment of NK cells toward BECs during bladder infections suggests that NK cells can recognize infected BECs. To validate this notion, we employed the human NK-92 cell line and the human 5637 BEC line to investigate potential molecular interactions between these two cell types. To mimic in vivo infection conditions, we first infected human BECs with the UPEC CI5 strain, followed by antibiotic treatment to eliminate all viable extracellular bacteria (Figure 2A). A significant reduction in bacterial load was observed when NK cells were added to the infected cells, compared to infected cells in the absence of NK cells (Figure 2B). Then, we examined whether this decrease in bacterial numbers in UPEC-infected BECs was dependent on NK cell-mediated cytotoxicity by assessing cell death using the LDH release assay (Broussas et al. 2013). A significant level of cellular cytotoxicity was observed when UPEC-infected BECs were co-incubated with NK cells (Figure 2C); however, these observations were absent without NK cells or when uninfected BECs were co-incubated with NK cells.

Since NK cells require cell-to-cell contact to induce target cell death, we employed microscopy to observe whether such cell-to-cell contact occurs. Indeed, direct contact between infected BECs and NK cells was evident when UPEC CI5-infected human 5637 BECs were exposed to NK-92 cells (Figure 2D). Interestingly, we observed that in many NK cells in contact with infected BECs, granzyme B appeared to have aggregated (Figure 2D, white arrowheads). This enzyme is typically produced in the cytosol of NK cells and only aggregates before being released to kill target cells. Meanwhile, the number of intercellular contacts between NK cells and infected BECs in the co-inhibition studies was significantly more frequent than those between NK cells and uninfected BECs (Figure 2D). Thus, NK cells appear to have the capacity to directly kill UPEC-infected BECs through physical contact, involving the discharge of granzyme-enriched granules.

UPEC infection of BECs induces a reduction in MHC-I inhibitory receptors

For UPEC-infected BECs to be recognized and killed by NK cells, certain inhibitory receptors on NK cells need to be inactivated, and correspondingly, certain activation receptors need to be engaged. Killer immunoglobulin-like receptors (KIRs) and NKG2A are inhibitory receptors on NK cells that recognize MHC-I molecules; when engaged, these receptors can prevent NK cell-mediated cytotoxicity (Anfossi et al. 2006). The downregulation of MHC-I expression on infected BECs represents one mechanism through which inhibitory receptors on NK cells can be inactivated. Thus, we examined MHC-I surface expression in UPEC-infected BECs using immunofluorescence microscopy. We observed that MHC-I surface expression was significantly reduced in UPEC-infected BECs compared to uninfected BECs (Figure 3A, white arrowheads). This infection-induced MHC-I downregulation on BECs was further confirmed by Western blot analysis of BECs exposed to different bacterial MOIs (Figure 3B). Additionally, after quantitatively examining mRNA levels of the MHC-I components *HLA-A*, *HLA-B*, and *HLA-C*, we observed that all three were downregulated in UPEC-infected BECs (Figure 3C). Therefore, UPEC infection downregulates MHC-I at both the protein and mRNA levels in BECs, potentially enabling NK cells to identify infected BECs as non-self-targets.

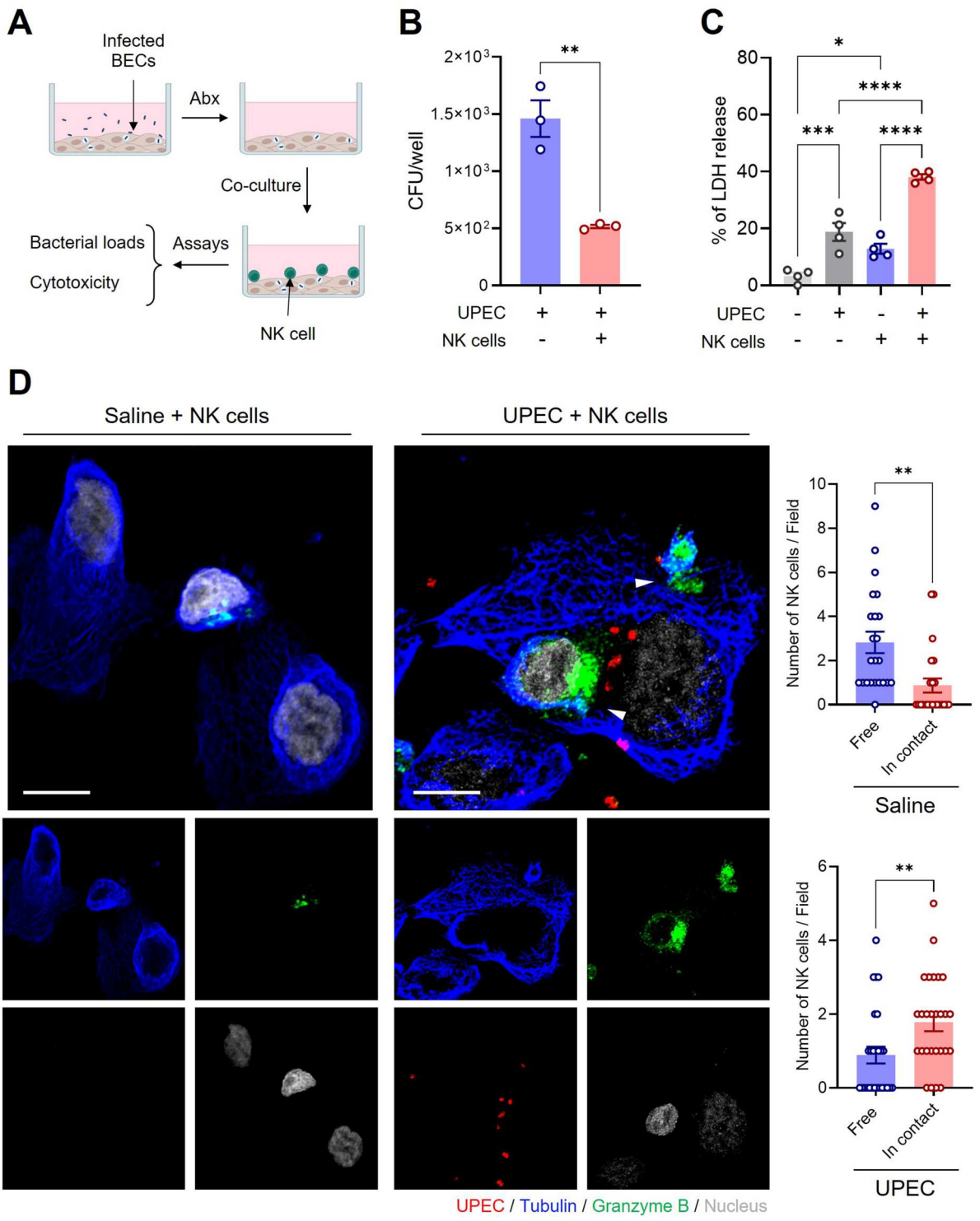


Figure 2. NK cells directly interacted with UPEC-infected BECs to reduce bacterial burden. (A) Schematic illustration of NK cell co-culture with UPEC-infected BECs. (B) NK cells reduced intracellular bacterial load in BECs. Human bladder 5637 cell line was infected with UPEC CI5 strain at an MOI of 200 for 24 h. NK cells were then incubated with the infected BECs in gentamicin-containing media for 16 h. Following incubation, intracellular bacterial loads were quantified. (C) Cytotoxicity assessment of NK cells against infected BECs. BECs were infected with UPEC for 24 h, followed by the addition of NK cells at a 1:1 ratio. After a 16-hour incubation, cytotoxicity was quantified by measuring LDH release from dying cells. (D) Direct physical contact formation between NK cells and infected BECs. Cells were stained for granzyme B (green), UPEC (red), tubulin (blue), and nucleus (gray). Synapse formation was captured using Z-stack imaging with confocal microscopy and quantified by counting the number of NK cells interacting with infected BECs within an optical field of 100 µm × 100 µm.

Data are shown as the mean ± SEM. Quantitative data from two to three independent experiments were analyzed by unpaired two-tailed Student's t-test or ordinary one-way ANOVA. * $p < 0.05$; ** $p < 0.01$; *** $p < 0.001$; **** $p < 0.0001$.

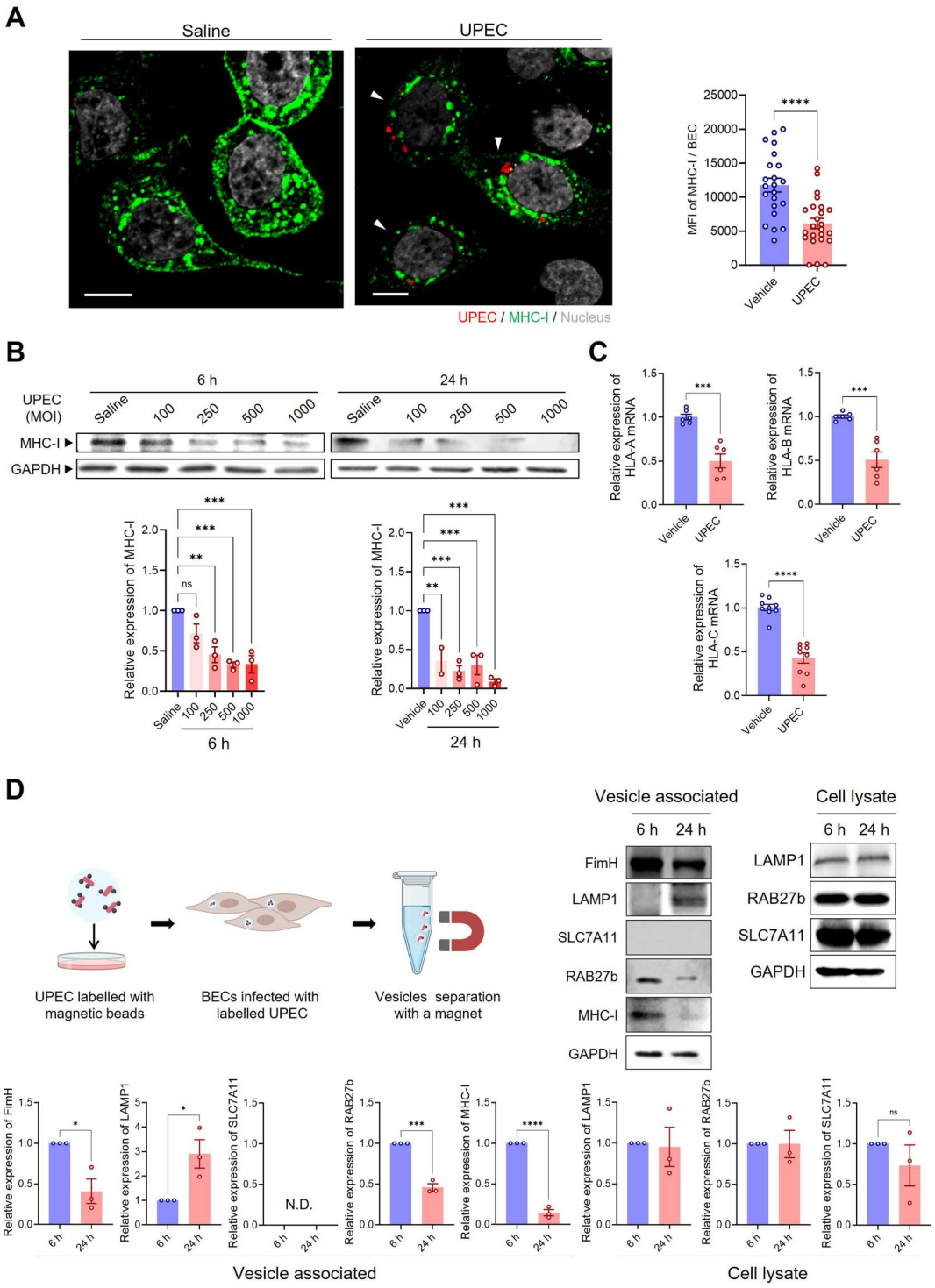


Figure 3. Infection of bladder epithelial cells by UPEC induces a reduction in MHC-I. (A) Reduction in MHC-I expression in BECs following UPEC infection. Cells were stained for MHC-I (green), UPEC (red), and DAPI (gray). The left panel shows saline-treated cells, while the right panel shows infected cells. MHC-I expression was assessed by mean fluorescence intensity. (B) To quantify MHC-I reduction, BECs were infected with UPEC at different MOIs (100, 200, 500, or 1000) and harvested at 6 and 24 h post-infection for Western blot analysis. GAPDH was used as a loading control. Densitometry analysis of MHC-I was performed using three independently conducted Western blot images. (C) Quantification of transcription levels post-infection. BECs were infected with UPEC at an MOI of 500. After 4 h of post-infection, qPCR was performed for *HLA-A*, *HLA-B*, or *HLA-C*. (D) Vesicle association of MHC-I after UPEC infection. BECs were infected with magnetic bead-labeled UPEC and harvested at 6 or 24 h post-infection. Samples were probed for various proteins (FimH, LAMP1, SLC7A11, RAB27b, or MHC-I) at different time points. The cell lysate fraction was also analyzed as the loading control.

Data are shown as the mean ± SEM. Quantitative data from two to three independent experiments were analyzed by unpaired two-tailed Student's t-test or ordinary one-way ANOVA. * $p < 0.05$; *** $p < 0.001$; **** $p < 0.0001$; n.s, not significant.

Internalization of MHC-1 and degradation in autolysosomes

Next, we investigated the underlying mechanism responsible for the sudden loss of cell surface MHC-I expression in UPEC-infected BECs. One potential explanation is that MHC-I is internalized along with receptors of UPEC adhesins when adherent UPEC is internalised by BECs, leading to its rapid reduction from the cell surface. Accordingly, the UPEC CI5 strain was labeled with magnetic beads as described previously (Naskar et al. 2023) and then exposed to monolayers of BECs. After 6 or 24 h of incubation, the plasma membrane of the BECs was disrupted, and the intracellular vesicles harboring internalized UPEC were isolated using a magnet and subjected to Western blot analysis (Figure 3D). At 6 h post-infection, labeled UPEC was detected, as expected, in vesicles highly enriched with RAB27b. Interestingly, these vesicles were also enriched with MHC-I (Figure 3D). When examining the intracellular compartments harboring labeled UPEC at 24 h post-infection, we again found that these compartments were highly enriched with LAMP1, an autolysosome marker known to harbor UPEC (Naskar et al. 2023). However, the levels of RAB27b and MHC-I were dramatically decreased within these autolysosomes (Figure 3D). Next, we examined the presence of SLC7A11, a plasma membrane-expressed transporter, in UPEC-containing vesicles via Western blotting to assess the specificity of the association between MHC-I and UPEC-harboring vesicles. Despite the abundance of SLC7A11 in whole-cell lysates, we found no indication of SLC7A11 within these vesicles (Figure 3D). These results suggest that MHC-I, expressed on the epithelial cell surface, is internalized by BECs in RAB27b$^+$ fusiform vesicles along with UPEC and is subsequently degraded within autolysosomal vesicles, thereby reducing surface expression.

MHC-I trafficking to autolysosomes involves the autophagy pathway

Since the movement of internalized UPEC from Rab27b-enriched vesicles to autolysosomes involves the autophagy pathway (Miao et al. 2015; Naskar et al. 2023), we investigated the role of this pathway in MHC-I degradation. Consequently, we used an inhibitor of V-ATPase, a proton pump located on the membranes of autophagosomes, which is essential for the autophagy-related breakdown of cargo. Our results showed that inhibiting V-ATPase successfully prevented MHC-I degradation (Figure 4A). A control experiment, in which UPEC-infected BECs were exposed to MG132, a proteasome inhibitor, revealed that MHC-I degradation still occurred, even at higher doses of the inhibitor (Figure 4A).

If the autophagy pathway is involved in MHC-I degradation, we would expect interactions between MHC-I and proteins associated with autophagosomes. Therefore, we used antibodies against LC3A/B to probe for these interactions in BECs at 8 h post-infection. We observed colocalization of intracellular MHC-I, LC3B, and UPEC (Figure 4B, yellow arrowhead), as well as multiple instances of colocalization between MHC-I and LC3B in the absence of bacteria (Figure 4B, white arrowhead). At 20 h post-infection, both MHC-I and intracellular UPEC appeared to colocalize with LAMP1, indicating that both cargos had been trafficked into autolysosomes (Figure 4B, yellow arrowhead). Interestingly, the colocalization of MHC-I with LAMP-1 appeared to occur independently of UPEC, as observed previously in the association of MHC-I with LC3B when MHC-I and LAMP-1 colocalization was detected in the absence of bacteria (Figure 4B, white arrowhead). Quantification of the colocalization between MHC-I and LC3B, as well as between MHC-I and LAMP1, using Pearson's coefficient scores, identified that both interactions were significant (Figure 4B). These findings suggest that MHC-I is internalized independently of UPEC into autophagosomes during UPEC infection of BECs, and is subsequently trafficked to LAMP1$^+$ lysosomal vesicles for autolysosomal degradation.

To further investigate whether the autophagy pathway contributes directly to MHC-I degradation, siRNA knockdown was applied to selectively reduce the expression of several autophagy-related components, including NBR1, BECLIN1, and ATG5, which are key proteins involved in phagophore formation and autophagosome maturation (Melia et al. 2020). Subsequently, we assessed how depleting these components altered MHC-I degradation in infected BECs. Compared to samples treated with scrambled (scr) siRNA, MHC-I degradation was prevented following NBR1, BECLIN1, or ATG5 knockdown (Figure 4C–E). These findings confirm that autophagy components play a crucial role in MHC-I degradation.

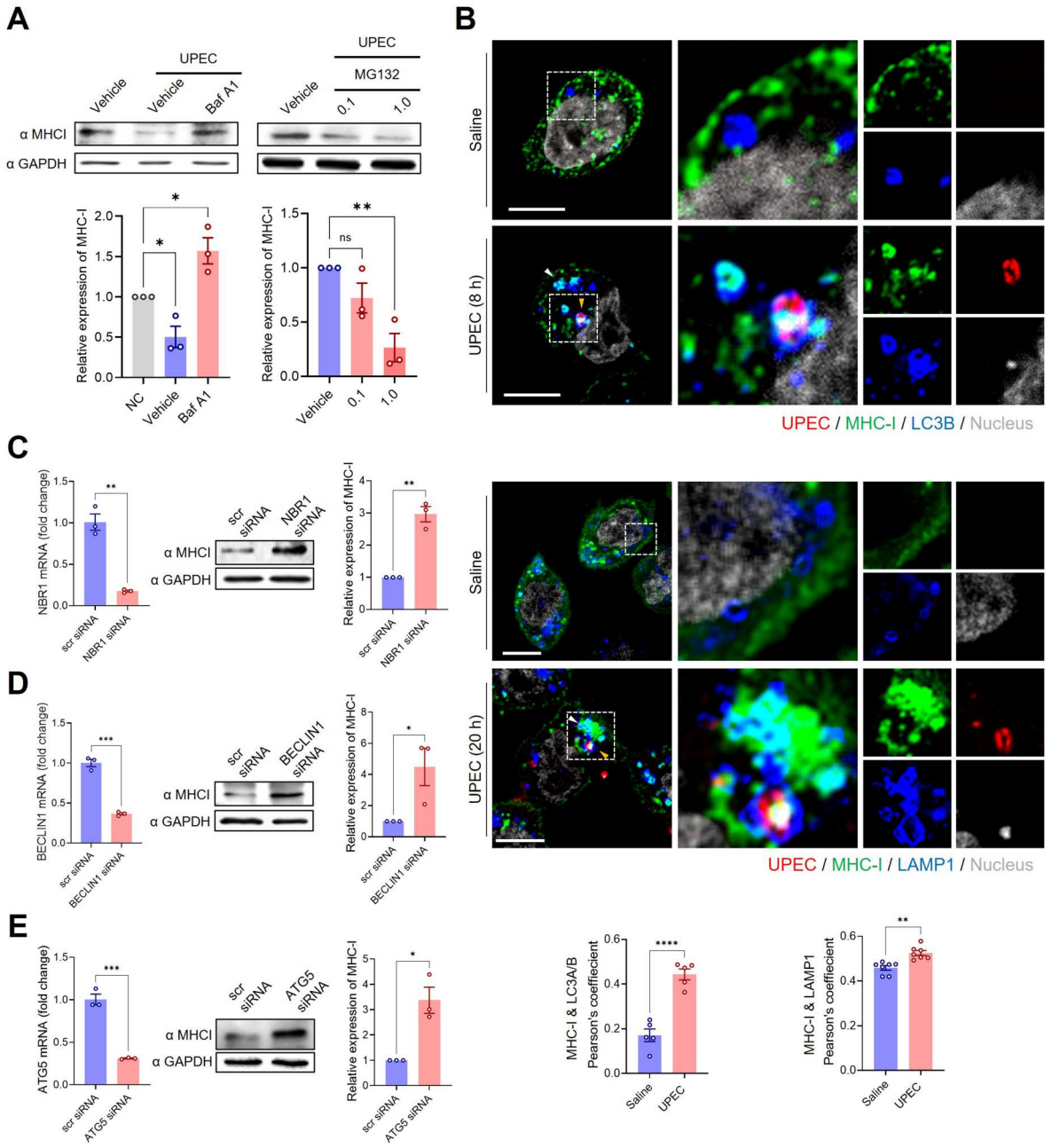


Figure 4. Autophagy-mediated degradation of MHC-I in UPEC-infected BECs. (A) Human BECs were treated with bafilomycin A1 (50 nM) or MG132 (0.1 μM or 1 μM) overnight. The following day, the cells were infected with UPEC at MOI 500 and subsequently probed for MHC-I expression via Western blot. The cells were harvested 24 h later and then probed for MHC-I via Western blot. GAPDH antibody was used as a control. Densitometry analysis of MHC-I was performed using three independently conducted Western blot images. (B) Confocal microscopy was performed to visualize the colocalization of MHC-I along with the intracellular vesicle components. The infected BECs with UPEC (MOI 200) were stained for LC3B (blue), UPEC (red), MHC-I (green), or the nucleus (gray). To visualize the colocalization of MHC-I with lysosomal vesicles, UPEC-infected cells were stained for LAMP1 (blue), UPEC (red), MHC-I (green), and nucleus (gray) after 20 h of infection. The regions outlined with white dashed lines in the panels of the first column are enlarged and shown in the remaining panels. Optical fields (100 μm × 100 μm) were randomly chosen from two to three independent experiments. Colocalization between the channels was measured in terms of Pearson's coefficient. (C, D, E) First, the siRNA knockdown efficacy of *NBR1*, *BECLIN1*, or *ATG5* was examined using qPCR. Then, BECs were again transfected with *NBR1*, *BECLIN1*, or *ATG5* siRNAs, followed by UPEC infection (MOI, 500). MHC-I levels were analyzed 24 h post-infection via Western blot. Densitometry analysis of MHC-I was performed using three independently conducted Western blot images.

Data are shown as the mean ± SEM. Quantitative data from two to three independent experiments were analyzed by unpaired two-tailed Student's t-test or ordinary one-way ANOVA. * $p < 0.05$; ** $p < 0.01$; *** $p < 0.001$; **** $p < 0.0001$; n.s, not significant.

CD48 upregulation in UPEC-infected BECs promotes NK cell-mediated attack

Notably, a reduction in MHC-I alone is insufficient for NK cells to effectively kill target cells; the engagement of NK cell-activating receptors by ligands on the target cell is also required (Long et al. 2013). Therefore, we investigated whether certain NK cell-activating receptor ligands are upregulated in UPEC-infected BECs. We compared the mRNA expression levels of several known NK cell-activating ligands in BECs, including MIC-A/-B, ULBP1-6, BAG, B7-H6, CD112, CD155, and CD48, before and after UPEC infection. While the expression of most tested ligands remained unchanged or decreased compared to uninfected BECs, CD48 exhibited close to a threefold increase following UPEC infection (Figure 5A). A corresponding increase in CD48 protein expression in UPEC-infected BECs was confirmed by Western blotting (Figure 5B). CD48 is a well-recognized ligand for the NK cell-activating receptor 2B4 (Garni-Wagner et al. 1993; Latchman et al. 1998; Zarama et al. 2014), particularly in the context of Epstein–Barr virus infections (Thorley-Lawson et al. 1982). To determine whether CD48 in UPEC-infected BECs facilitated NK cell targeting and subsequent bacterial clearance, *CD48* knockdown was conducted in human 5637 BECs, while control BECs were treated with scrambled siRNA (Figure 5C). After confirming CD48 knockdown, two different concentrations of *CD48* siRNA or scr siRNA

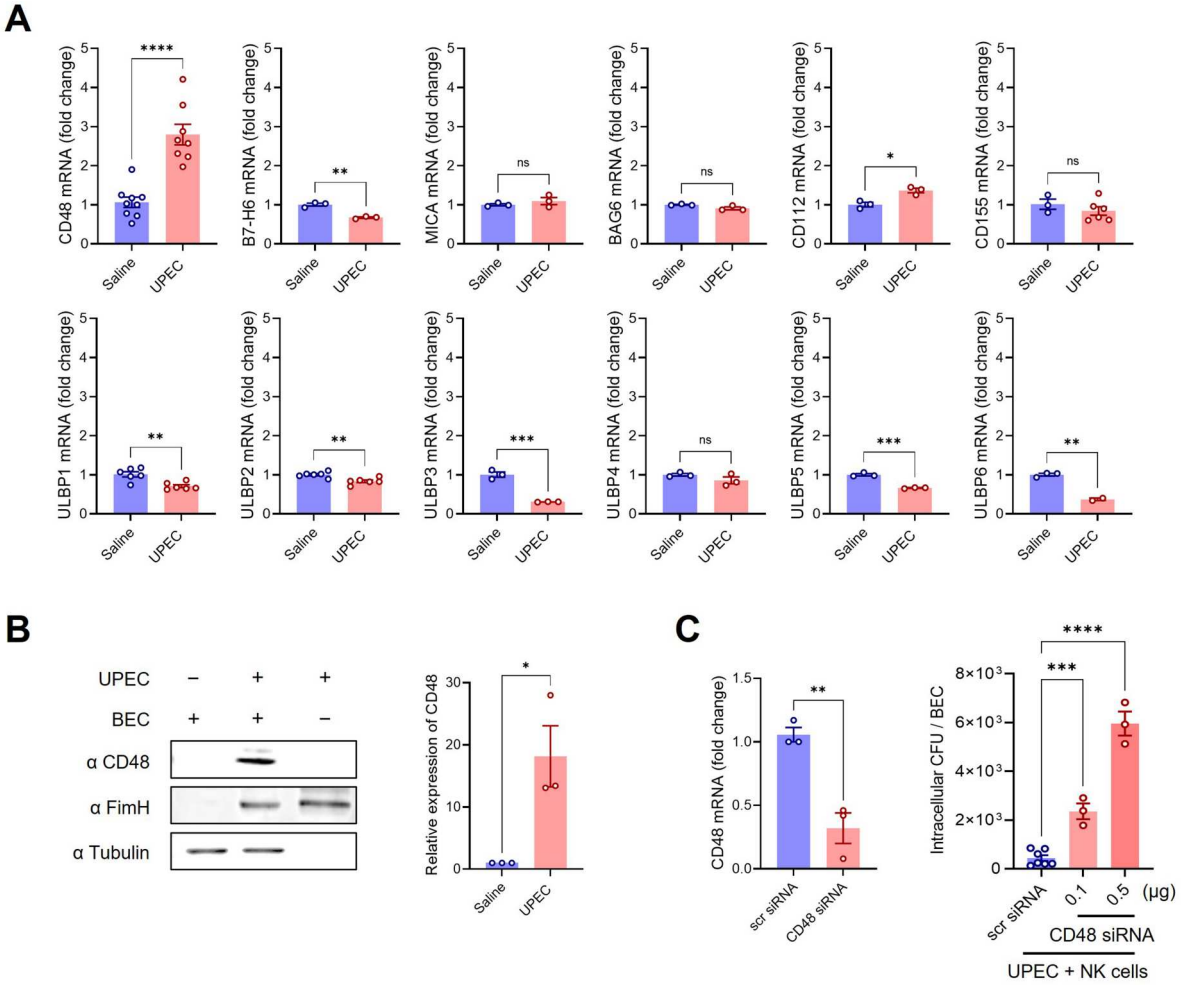


Figure 5. CD48 upregulation in UPEC-infected bladder epithelial cells promotes NK cell activation and the elimination of target cells. (A) Activation ligand expression in infected BECs. The harvested cells were analyzed for elevated expression levels of known activation ligands (CD48, B7-H6, MICA, BAG6, CD112, CD155, ULBP1, ULBP2, ULBP3, ULBP4, ULBP5, or ULBP6) using qPCR. (B) The CD48 protein level was measured 24 h after UPEC infection using Western blot analysis. Densitometry analysis of CD48 was performed using three independently conducted Western blot images. (C) First, the *CD48* siRNA (0.5 μg) knockdown efficacy was examined using qPCR. Then, before UPEC infection, BECs were transfected with si*CD48*, followed by infection with UPEC (MOI 500). After 24 h, NK cells were added and co-incubated overnight. The next day, the bacterial burden was assessed.

Data are shown as the mean ± SEM. Quantitative data from two to three independent experiments were analyzed by unpaired two-tailed Student's t-test or ordinary one-way ANOVA. * $p < 0.05$; ** $p < 0.01$; *** $p < 0.001$; **** $p < 0.0001$; n.s, not significant.

were applied to BECs, which were then infected with UPEC and exposed to NK cells. Bacterial burden within BECs was then measured. The capacity of NK cells to reduce the bacterial burden in infected BECs was markedly diminished in BECs with reduced CD48 expression (Figure 5C). Therefore, CD48 expression on UPEC-infected BECs is essential to trigger NK cell-mediated bacterial clearance.

CXCL10 and CXCL12 promote NK cell recruitment to UPEC-infected BECs

To understand how NK cells are recruited to BECs to promote bacterial killing, we investigated whether BECs secrete specific chemotactic factors in response to infection. To examine this in vitro, we utilized a Transwell co-culture system with a 5.0 μm pore size, which is sufficient to allow NK cell migration but prevents BEC movement. NK cells were introduced into the upper chamber of the Transwell system, and their migration toward plated UPEC-infected BECs in the lower chamber was assessed by examining cells in the lower chamber after overnight incubation (Figure 6A). To distinguish NK cells from BECs in the lower chamber, we stained for granzyme B-positive cells. We found that many NK cells had successfully transmigrated and joined UPEC-infected BECs (Figure 6A). To identify the specific chemokine signals responsible for NK cell recruitment to infected BECs, we performed qPCR analysis for *CCL5*, *CCL19*, *CX3CL1*, *CXCL10*, and *CXCL11*, chemokines previously implicated in NK cell attraction by various cell types. While the expression levels of most chemokines were either slightly increased or remained unchanged following infection, the expression of *CXCL10* and *CXCL12* was significantly increased (Figure 6B).

Next, we investigated the functional role of these upregulated chemokines by examining whether CXCL10 and CXCL12 knockdown could affect NK cell migration toward UPEC-infected BECs in Transwell assays. Using CRISPR–Cas9 technology, we created $CXCL10^{-/-}$, $CXCL12^{-/-}$, and control $CXCL9^{-/-}$ BECs, and conducted co-culture experiments. Compared to infected wild-type and $CXCL9^{-/-}$ BECs, UPEC-infected $CXCL10^{-/-}$ and $CXCL12^{-/-}$ BECs did not recruit NK cells (Figure 6C). These results indicate that CXCL10 and CXCL12 are crucial for facilitating NK cell recruitment to UPEC-infected BECs by promoting transmigration across the endothelial barrier.

Therapeutic targeting of NK cells to combat UPEC infections in the bladder

The persistence of intracellular UPEC in the bladder is considered a significant factor in the recurrence of UTIs. Given the recent success of NK cell-directed therapies in treating viral infections (Strauss-Albee et al. 2015), we investigated the potential of NK cells in eliminating intracellular bacteria.

Interleukin-15 (IL-15) is a critical cytokine for the development and function of NK cells; meanwhile, IL-15 exposure has been shown to significantly enhance NK cell proliferation, cytotoxic activity, and interferon-γ production (Lodolce et al. 1998; Kennedy et al. 2000). This study aimed to investigate the therapeutic benefits of administering exogenous IL-15 in our UTI infection model. Notably, IL-15 exhibits greater biological activity when presented in complex with the IL-15 receptor α (IL-15Rα) subunit, as this configuration extends the cytokine half-life and improves biodistribution (Rubinstein et al. 2006). Therefore, we utilized the IL-15:IL-15Rα complex instead of standard recombinant IL-15.

We first assessed the effects of i.p. administration of the IL-15:IL-15Rα complex (0.5 μg of IL-15 and 3 μg of IL-15Rα) on NK cell levels in WT C57BL/6J mice. Even in the absence of an infection, the number of $NK1.1^{+}$ $NKp46^{+}$ $CD45^{+}$ $CD3\varepsilon^{-}$ $CD19^{-}$ NK cells significantly increased in various tissues following IL-15:IL-15Rα complex administration (Figure 7A). This increase was observed in the bloodstream, the bladder, and spleen (Figure 7A). Therefore, we infected the bladders of mice with UPEC, followed by antibiotic treatment to eliminate extracellular bacteria. After 24 h, we administered the IL-15:IL-15Rα complex via i.p. injection, and 3 days post-infection, we measured the bacterial load in the bladder. Mice treated with the IL-15:IL-15Rα complex exhibited a significantly reduced bacterial load compared to the control group (Figure 7B). Thus, NK cell activation through the IL-15:IL-15Rα complex enhances bacterial clearance in the bladder during UTIs, highlighting the antibacterial role of NK cells and the potential of NK cell-targeted therapy as an adjunct to current treatments.

Discussion

Growing evidence suggests that recurrent UTIs are, at least in part, attributable to the persistence of UPEC in a quiescent phase within BECs, even after the initial infection has subsided (Anderson et al. 2003; Mysorekar

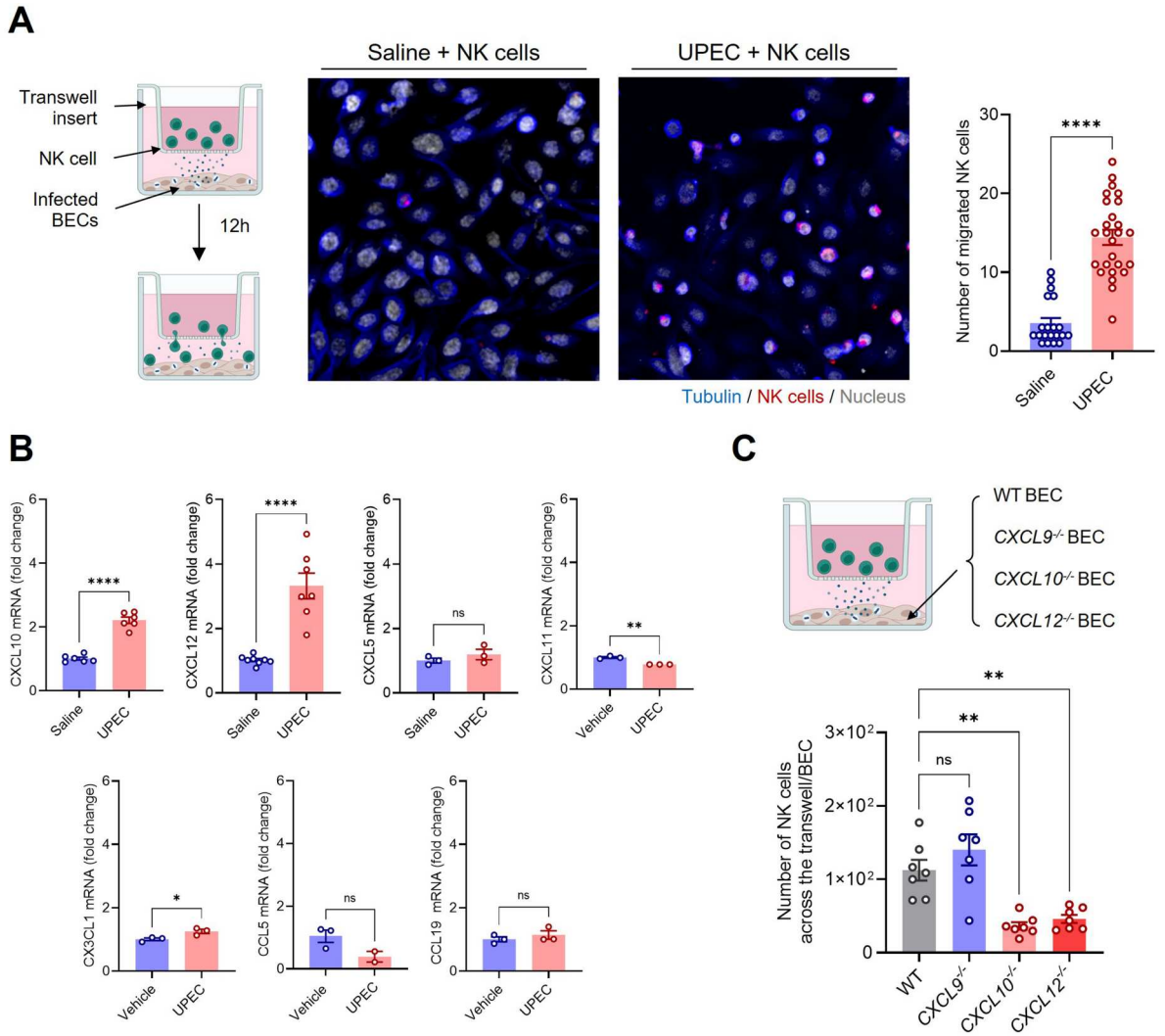


Figure 6. CXCL10 and CXCL12 mediate NK cell recruitment to UPEC-infected bladder epithelial cells. (A) NK cell migration through a Transwell plate. Cells were fixed and stained for granzyme B (red), nucleus (gray), and tubulin (blue). The number of transmigrated NK cells was counted and compared. Optical fields (100 μm × 100 μm) were randomly chosen from two to three independent experiments. (B) Enhanced expression of chemokine transcription for NK cell recruitment. Transcription levels of *CXCL10*, *CXCL12*, *CXCL5*, *CXCL11*, *CXCL1*, *CCL5*, or *CCL19* were measured via qPCR after BECs were infected with UPEC for 24 h. (C) CXCL10 and CXCL12 are required to recruit NK cells in the Transwell. *CXCL9*$^{-/-}$, *CXCL10*$^{-/-}$, or *CXCL12*$^{-/-}$ BECs were generated by CRISPR–Cas9. These knockout cells or mock control BECs were infected with UPEC (MOI 200) and plated on the basal well of the Transwell insert. Transmigrated NK cells were compared by counting cells in the basolateral side of the Transwell system.

Data are shown as the mean ± SEM. Quantitative data from two to three independent experiments were analyzed by unpaired two-tailed Student's t-test or ordinary one-way ANOVA. * $p < 0.05$; ** $p < 0.01$; **** $p < 0.0001$.

and Hultgren 2006; Miao et al. 2015; Naskar et al. 2023). Since BECs are long-lived, these cells can act as reservoirs for bladder reinfection over extended periods, particularly after antibiotic treatments. Within their intracellular niche, UPEC are protected from both antibiotics and host immune responses, including the antimicrobial actions of soluble factors such as complement and antimicrobial peptides, as well as phagocytic cells that typically clear extracellular bacteria (Naskar and Choi 2024). Given this situation, identifying immune mechanisms within the bladder that have the potential to target and eliminate this intracellular niche of UPEC is crucial. Thus, this study proposes that NK cells eliminate intracellular UPEC through the downregulation of MHC-I, a concept illustrated in Figure 7C.

This study demonstrated the crucial role of NK cells in targeting bacteria-harboring BECs and reducing bacterial load in the bladder following UTIs. We found that significant numbers of NK cells were recruited

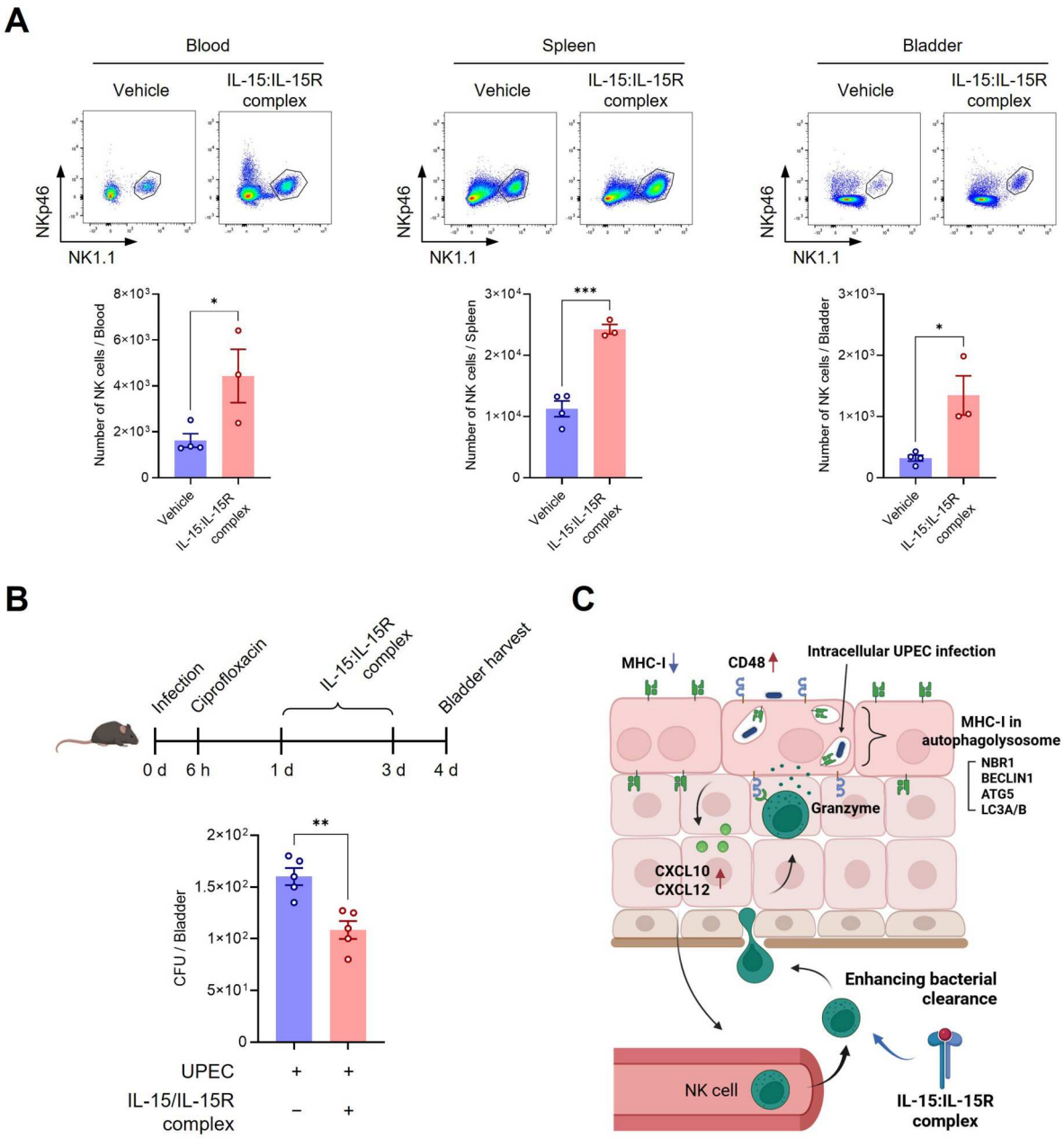


Figure 7. Therapeutic potential of the IL-15:IL-15Rα complex in NK cell activation to combat persistent UPEC infections in the bladder. (A) Stimulation of NK cells was conducted twice via i.p. injection of the IL-15:IL-15Rα complex. The complex consisted of 0.50 μg IL-15 and 3 μg of IL-15Rα. Mice bladders, blood, and spleens were harvested 24 h after the second dose and analyzed via flow cytometry to assess the increase in NK cell number. (B) The difference in bacterial burden in mice following the above-mentioned model was assessed by measuring the bacterial load in the bladder. The mice were first administered two doses of the IL-15:IL-15Rα complex, followed by 1×10^8 CFU of UPEC CI5 strain and ciprofloxacin treatment. Bacterial burden was measured. Each dot represents an individual mouse, and the panel shows the combined results from two or three independent experiments.

Data are shown as the mean ± SEM. Quantitative data from two to three independent experiments were analyzed by unpaired two-tailed Student's t-test. * $p < 0.05$; ** $p < 0.01$; *** $p < 0.001$.

into the lamina propria and superficial epithelium as early as 4 h after the initiation of a UTI, with their numbers peaking at 8 h and diminishing by 24 h, possibly coinciding with the clearance of most of the infecting bacteria. The crucial role of NK cells in bacterial clearance, particularly of intracellular bacteria, was demonstrated by the limited bacterial clearance observed in UTI mice, which had been depleted of NK cells using an antibody, compared to mice administered the control antibody. Our in vitro studies

suggest that NK cells mediate bacterial clearance by migrating toward bacteria-harboring BECs, directly binding to infected cells, and subsequently releasing a focal discharge of granules enriched in granzyme B, a serine protease that promotes programmed cell death in target cells (Bjorkstrom et al. 2022). The recruitment of NK cells was found to be driven by BEC-secreted chemotactic factors. Only CXCL10 and CXCL12 were selectively produced among the known NK chemokines. The crucial role of CXCL10 and CXCL12 was demonstrated by knocking out the expression of either chemokine, which resulted in the abrogation of NK cell migration toward UPEC-infected BECs.

The downregulation of cell-surface MHC-I molecules represents a critical factor known to promote the targeting of infected host cells by NK cells (Halenius et al. 2015). We found that the association of NK cells with infected BECs was also linked to the widespread downregulation of MHC-I expression on the infected BECs. Furthermore, we observed that MHC-I downregulation was dose-dependent, with higher bacterial doses inducing greater reduction in MHC-I expression. Interestingly, the reduction in cell-surface MHC-I expression in infected BECs involved the internalization of MHC-I molecules, followed by their degradation within autolysosomes. This process was mediated by the encapsulation of MHC-I within Rab27B$^+$ vesicles, which were subsequently transferred into autophagosomes and then into autolysosomes. This trafficking pathway required the active participation of autophagy components NBR1, BECLIN1, and ATG5. A similar autophagy-dependent degradation of MHC-I has also been reported in cancer, where MHC-I molecules are selectively recognized by cargo receptors, such as NBR1, and subsequently degraded, thereby enabling tumor cells to evade cytotoxic T cell-mediated responses (Yamamoto et al. 2020). Although MHC-I degradation yields distinct physiological outcomes in infection and cancer, degradation through the autophagy pathway underscores a shared principle in which the process serves as a pivotal regulator of cellular fate and immune interactions.

Notably, this meandering internalization route of MHC-I in BECs closely resembles that described for UPEC, wherein bacteria are first shuttled into Rab27B$^+$ fusiform vesicles before being enclosed in autophagosomes and ultimately degraded within autolysosomes (Flores-Mireles et al. 2015). The similarity in the internalization pathways of UPEC and MHC-I suggests that MHC-I uptake may be triggered by UPEC uptake. Support for this notion was noted in the microscopic findings, whereby UPEC colocalized with MHC-I within autophagosomes of BECs. However, the frequent presence of MHC-I within autophagosomes, even in the absence of UPEC, would suggest that MHC-I trafficking into autophagosomes is not necessarily dependent on bacterial infection. In addition to the active removal of MHC-I from the cell surface, we found the general reduction in MHC-I levels in infected BECs is attributable to decreased transcription and expression of new MHC-I proteins, through as yet unknown mechanisms. These multifaceted activities aimed at reducing MHC-I expression parallel those observed in virus-infected cells, where the synthesis, translation, and/or trafficking of MHC-I to the cell surface is hindered through various mechanisms.

Concomitant with the downregulation of MHC-I on infected BECs, we observed the selective upregulation of CD48 expression among other known NK cell activators on BECs. CD48 knockdown in BECs was also shown to reduce NK cell-mediated killing of intracellular UPEC. CD48 is a glycosylphosphatidylinositol (GPI)-anchored glycoprotein, and its presence on the cell surface of BECs can promote NK cell attachment and activation through specific coupling with its commentary ligand, CD244 (Latchman et al. 1998). Thus, while the presence of MHC-I on host cells signals NK cells not to target them, CD48 expression on the same cells serves to 'activate' NK cells, prompting them to target the infected cells via the release of cytotoxic granules containing granzyme B. This NK cell-mediated targeting of UPEC-infected BECs aligns with traditional NK cell mechanisms for eliminating various virus-infected host cells (Bjorkstrom et al. 2022). Interestingly, CD48 has previously been identified as a putative receptor for the attachment of FimH-expressing *E. coli* to immune cells, including macrophages and mast cells (Malaviya et al. 1999). Presumably, when CD48 is upregulated in UPEC-infected BECs, it may not only enhance NK cell binding but also facilitate the adhesion of additional UPEC to the epithelial surface.

Although we have observed a significant contribution of NK cells to bacterial clearance, the magnitude of this effect was moderate, as indicated by the differences in bacterial counts between mice administered the control antibody and those treated with the NK cell-depleting antibody. Nonetheless, our findings contradict earlier studies that reported no change in bacterial burden in the bladders of UTI mice following NK cell depletion with antibodies (Gur et al. 2013). We believe the discrepancy between our findings and those of previous studies arises from our exclusive focus on intracellular bacterial counts, which were assessed

following antibiotic treatment of the bladders. Our rationale for emphasizing intracellular bacteria during infection is based on the understanding that NK cells primarily target these intracellular pathogens. Previously, the presence of large numbers of extracellular bacteria, which often adhere to the surfaces of infected BECs, may have obscured any potential NK cell-mediated reduction in intracellular bacterial numbers.

While a significant number of women experience UTIs, only a minority develop recurrent infections. This observation highlights the robustness of the multifaceted immune system in hosts and suggests that recurrent UTIs may result from defects in one or more of the immune components (Naskar and Choi 2024). Since NK cell levels can fluctuate based on the immune status of an individual, a potential determinant of whether UPEC persists in BECs after a UTI may be the number of recruited NK cells and their level of activity. Older patients, a population well known to possess reduced NK cell levels and activity (Brauning et al. 2022), exhibit a higher rate of recurrent UTIs, which supports this hypothesis (Foxman and Brown 2003; Eriksson et al. 2010).

Whenever possible, we have complemented our in vivo mouse studies with in vitro studies using human cells or specimens to enhance the relevance of our research. Our findings with human BECs and NK cells align with our observations in mice. Additionally, we demonstrated NK cell activity in patients by detecting NK cell-derived granzymes in the urine of UTI patients, whereas these granzymes were absent in control samples. Given the promise of NK cell-targeting therapies in combating viral infections in patients (Schmidt et al. 2018), we tested the efficacy of treating mice that had recently been infected with UPEC by administering an i.p. injection of the IL-15:IL-15Rα complex, which is known to activate and promote NK cell expansion. Our results revealed that this treatment significantly improved bacterial clearance from the bladder, suggesting that targeted enhancement of NK cell activity could facilitate the elimination of UPEC. This finding is especially relevant because a major limitation in NK cell effectiveness against UPEC is their recruitment into the bladder only during active infection, with their numbers rapidly diminishing once the primary infection has resolved. Consequently, NK cells are not present to eliminate residual pockets of UPEC-infected BECs after each UTI. If NK cell recruitment into the bladder could be actively induced after UTIs have resolved – potentially through the use of formulations such as IL-15:IL-15Rα – these residual bacterial pockets could be more effectively eliminated, thereby reducing the risk of recurrent UTIs.

Acknowledgements

We thank our collaborators for reviewing this manuscript and for their suggestions. **Manisha Naskar:** Conceptualization, Methodology, Formal analysis, Writing – Original Draft. **Gyeongseo Suk:** Methodology, Formal analysis. **Hana Yoon:** Resources, Writing – Review & Editing. **Donghoon Lim:** Writing – Review & Editing. **Soman N. Abraham**: Writing – Review & Editing. ***Hae Woong Choi***: Conceptualization, Methodology, Formal analysis, Writing – Original Draft, Supervision, Funding acquisition.

Disclosure statement

No potential conflict of interest was reported by the authors.

Funding

This work was supported by the National Research Foundation of Korea [grant numbers NRF-2020R1C1C1003257, RS-2023-00221182, and RS-2025-00515944] and the internal grant of Korea University.

Data availability statement

The corresponding author can provide source data that support the findings of this study upon request.

ORCID

Hae Woong Choi http://orcid.org/0000-0001-9372-1875

References

Abraham SN et al. 1985. Protection against *Escherichia coli*-induced urinary tract infections with hybridoma antibodies directed against type 1 fimbriae or complementary D-mannose receptors. Infect Immun. 48(3):625–628. https://doi.org/10.1128/iai.48.3.625-628.1985

Anderson GG et al. 2003. Intracellular bacterial biofilm-like pods in urinary tract infections. Science. 301(5629):105–107. https://doi.org/10.1126/science.1084550

Anfossi N et al. 2006. Human NK cell education by inhibitory receptors for MHC class I. Immunity. 25(2):331–342. https://doi.org/10.1016/j.immuni.2006.06.013

Bishop BL et al. 2007. Cyclic AMP-regulated exocytosis of *Escherichia coli* from infected bladder epithelial cells. Nat Med. 13(5):625–630. https://doi.org/10.1038/nm1572

Bjorkstrom NK, Strunz B, Ljunggren HG. 2022. Natural killer cells in antiviral immunity. Nat Rev Immunol. 22(2):112–123. https://doi.org/10.1038/s41577-021-00558-3

Brauning A et al. 2022. Aging of the immune system: focus on natural killer cells phenotype and functions. Cells. 11(6):1017. https://doi.org/10.3390/cells11061017

Broussas M, Broyer L, Goetsch L. 2013. Evaluation of antibody-dependent cell cytotoxicity using lactate dehydrogenase (LDH) measurement. Methods Mol Biol. 988:305–317. https://doi.org/10.1007/978-1-62703-327-5_19

Chen Y et al. 2003. Rab27b is associated with fusiform vesicles and may be involved in targeting uroplakins to urothelial apical membranes. Proc Natl Acad Sci U S A. 100(24):14012–14017. https://doi.org/10.1073/pnas.2436350100

Choi HW et al. 2016. Loss of bladder epithelium induced by cytolytic mast cell granules. Immunity. 45(6):1258–1269. https://doi.org/10.1016/j.immuni.2016.11.003

Eriksson I, Gustafson Y, Fagerstrom L, Olofsson B. 2010. Prevalence and factors associated with urinary tract infections (UTIs) in very old women. Arch Gerontol Geriatr. 50(2):132–135. https://doi.org/10.1016/j.archger.2009.02.013

Flores-Mireles AL, Walker JN, Caparon M, Hultgren SJ. 2015. Urinary tract infections: epidemiology, mechanisms of infection and treatment options. Nat Rev Microbiol. 13(5):269–284. https://doi.org/10.1038/nrmicro3432

Foxman B, Brown P. 2003. Epidemiology of urinary tract infections: transmission and risk factors, incidence, and costs. Infect Dis Clin North Am. 17(2):227–241. https://doi.org/10.1016/S0891-5520(03)00005-9

Garni-Wagner BA, Purohit A, Mathew PA, Bennett M, Kumar V. 1993. A novel function-associated molecule related to non-MHC-restricted cytotoxicity mediated by activated natural killer cells and T cells. J Immunol. 151(1):60–70. https://doi.org/10.4049/jimmunol.151.1.60

Gur C et al. 2013. Natural killer cell-mediated host defense against uropathogenic E. coli is counteracted by bacterial hemolysinA-dependent killing of NK cells. Cell Host Microbe. 14(6):664–674. https://doi.org/10.1016/j.chom.2013.11.004

Halenius A, Gerke C, Hengel H. 2015. Classical and non-classical MHC I molecule manipulation by human cytomegalovirus: so many targets-but how many arrows in the quiver? Cell Mol Immunol. 12(2):139–153. https://doi.org/10.1038/cmi.2014.105

Justice SS, Hunstad DA, Seed PC, Hultgren SJ. 2006. Filamentation by *Escherichia coli* subverts innate defenses during urinary tract infection. Proc Natl Acad Sci U S A. 103(52):19884–19889. https://doi.org/10.1073/pnas.0606329104

Kärre K, Ljunggren HG, Piontek G, Kiessling R. 1986. Selective rejection of H-2-deficient lymphoma variants suggests alternative immune defence strategy. Nature. 319(6055):675–678. https://doi.org/10.1038/319675a0

Kennedy MK et al. 2000. Reversible Defects in Natural Killer and Memory Cd8 T Cell Lineages in Interleukin 15–Deficient Mice. J Exp Med. 191(5):771–780. https://doi.org/10.1084/jem.191.5.771

Koch J, Steinle A, Watzl C, Mandelboim O. 2013. Activating natural cytotoxicity receptors of natural killer cells in cancer and infection. Trends Immunol. 34(4):182–191. https://doi.org/10.1016/j.it.2013.01.003

Latchman Y, McKay PF, Reiser H. 1998. Identification of the 2B4 molecule as a counter-receptor for CD48. J Immunol. 161(11):5809–5812. https://doi.org/10.4049/jimmunol.161.11.5809

Lodolce JP et al. 1998. IL-15 receptor maintains lymphoid homeostasis by supporting lymphocyte homing and proliferation. Immunity. 9(5):669–676. https://doi.org/10.1016/S1074-7613(00)80664-0

Long EO, Kim HS, Liu D, Peterson ME, Rajagopalan S. 2013. Controlling natural killer cell responses: integration of signals for activation and inhibition. Annu Rev Immunol. 31:227–258. https://doi.org/10.1146/annurev-immunol-020711-075005

Malaviya R, Gao Z, Thankavel K, van der Merwe PA, Abraham SN. 1999. The mast cell tumor necrosis factor alpha response to FimH-expressing Escherichia coli is mediated by the glycosylphosphatidylinositol-anchored molecule CD48. Proc Natl Acad Sci USA. 96(14):8110–8115. https://doi.org/10.1073/pnas.96.14.8110

Melia TJ, Lystad AH, Simonsen A. 2020. Autophagosome biogenesis: from membrane growth to closure. J Cell Biol. 1(6):219.

Miao Y, Li G, Zhang X, Xu H, Abraham SN. 2015. A TRP channel senses lysosome neutralization by pathogens to trigger their expulsion. Cell. 161(6):1306–1319. https://doi.org/10.1016/j.cell.2015.05.009

Mysorekar IU, Hultgren SJ. 2006. Mechanisms of uropathogenic *Escherichia coli* persistence and eradication from the urinary tract. Proc Natl Acad Sci USA. 103(38):14170–14175. https://doi.org/10.1073/pnas.0602136103

Naskar M, Choi HW. 2024. A Dynamic interplay of innate immune responses during urinary tract infection. Immune Netw. 24(4):e31. https://doi.org/10.4110/in.2024.24.e31

Naskar M et al. 2023. alpha-Hemolysin promotes uropathogenic *E. coli* persistence in bladder epithelial cells via abrogating bacteria-harboring lysosome acidification. PLoS Pathog. 19(5):e1011388. https://doi.org/10.1371/journal.ppat.1011388

Rubinstein MP et al. 2006. Converting IL-15 to a superagonist by binding to soluble IL-15Rα. Proc Natl Acad Sci USA. 103(24):9166–9171. https://doi.org/10.1073/pnas.0600240103

Schmidt S, Tramsen L, Rais B, Ullrich E, Lehrnbecher T. 2018. Natural killer cells as a therapeutic tool for infectious diseases - current status and future perspectives. Oncotarget. 9(29):20891–20907. https://doi.org/10.18632/oncotarget.25058

Strauss-Albee DM et al. 2015. Human NK cell repertoire diversity reflects immune experience and correlates with viral susceptibility. Sci Transl Med. 7(297):297ra115.

Thorley-Lawson DA, Schooley RT, Bhan AK, Nadler LM. 1982. Epstein-Barr virus superinduces a new human B cell differentiation antigen (B-LAST 1) expressed on transformed lymphoblasts. Cell. 30(2):415–425. https://doi.org/10.1016/0092-8674(82)90239-2

Yamamoto K et al. 2020. Autophagy promotes immune evasion of pancreatic cancer by degrading MHC-I. Nature. 581(7806):100–105. https://doi.org/10.1038/s41586-020-2229-5

Yannaraki M et al. 2006. Urinary cytotoxic molecular markers for a noninvasive diagnosis in acute renal transplant rejection. Transpl Int. 19(9):759–768. https://doi.org/10.1111/j.1432-2277.2006.00351.x

Zarama A et al. 2014. Cytomegalovirus m154 hinders CD48 cell-surface expression and promotes viral escape from host natural killer cell control. PLoS Pathog. 10(3):e1004000. https://doi.org/10.1371/journal.ppat.1004000